Forest Ecology and Management 608 (2026) 123602

Contents lists available at ScienceDirect

Forest Ecology and Management

journal homepage: www.elsevier.com/locate/foreco

Contrasting cambial phenology and xylogenesis of southern and northern tree species in a boreal–temperate ecotone

Junzhou Zhang [a,b,c,*], Yiping Zhang [b,d,**], Min Li [a,c], Junliang Xu [d], Tessa Mandra [b], Keyan Jiang [a,c], David Orwig [b], Neil Pederson [b]

[a] Key Laboratory of Western China's Environmental Systems (Ministry of Education), College of Earth and Environmental Sciences, Lanzhou University, Lanzhou 730030, China
[b] Harvard Forest, Harvard University, 324 N Main St, Petersham, MA 01366, USA
[c] Gansu Liancheng Forest Ecosystem Field Observation and Research Station, Lanzhou University, Lanzhou 730333, China
[d] College of Horticulture and Plant Protection, Henan University of Science and Technology, Luoyang 471003, China

ARTICLE INFO

Keywords:
Climate change
Harvard Forest
Microcoring
Mixed forests
Transitional zones
Wood formation

ABSTRACT

Ecotones are highly sensitive to climate change, yet the growth responses of many tree species in these transitional zones remain understudied. We investigated cambial phenology and intra-annual radial growth in three southern (*Quercus alba*, *Carya ovata*, *Betula lenta*) and three northern (*Betula papyrifera*, *Picea rubens*, *Larix laricina*) species during 2019 and early 2020. Southern species achieved greater radial growth than northern species, despite similar growth durations. *Q. alba* initiated cambial activity roughly one month earlier than all other species, while peak growth for all but *Q. alba* occurred near the summer solstice. Following the cooler January–May period in 2019 compared with 2020, all species except *Q. alba* began growth approximately two weeks later. Phenology and growth dynamics were significantly influenced by tree size, wood type, and canopy position, with larger canopy trees sustaining cell production later into the season. Our findings suggest that these groups adopt distinct growth strategies: southern species rely on water-limited adaptations, whereas northern species are more temperature-limited. These findings provide new insights into species-specific growth strategies and climate responses in mixed boreal–temperate forests within ecotones. These mechanistic insights into how species with contrasting biogeographic origins and anatomies coordinate their growth under shared conditions refine our understanding of tree-climate interactions, making them crucial for the management and conservation of forests in ecotones.

1. Introduction

Ecotones are dynamic transition zones where forest ecosystems and species may be particularly susceptible to distributional shifts under climate change (Kark, 2013). These regions often host mixed assemblages of coniferous and deciduous species, with vegetation patterns shaped by temperature, precipitation, and disturbance regimes (FAO, 2020). As biodiversity hotspots positioned near the climatic tolerance limits of many species, transitional forests can exhibit heightened sensitivity to environmental change (Hansen et al., 2001). Southern temperate species such as oaks typically display greater thermal plasticity but reduced cold tolerance, whereas northern boreal species such as spruce show the opposite trend (Fei et al., 2017). Climate projections suggest that southern species will migrate northward, compressing the southern range limits of northern species and intensifying interspecific competition (Lenoir et al., 2008). Yet, empirical observations indicate that many southern species have not yet demonstrated clear northward shifts (Song et al., 2023). Within transition zones, southern species often achieve faster growth under moderate warming but face tradeoffs, including increased vulnerability to frost and drought due to high hydraulic efficiency (Charrier et al., 2021). In contrast, slower-growing boreal species are more resistant to shorter climatic fluctuations but may be disadvantaged under prolonged warming (Li et al., 2023; Martinez-Sancho et al., 2017). Advancing our understanding of

* Corresponding author at: Key Laboratory of Western China's Environmental Systems (Ministry of Education), College of Earth and Environmental Sciences, Lanzhou University, Lanzhou 730030, China.
** Corresponding author at: College of Horticulture and Plant Protection, Henan University of Science and Technology, Luoyang 471003, China.
E-mail addresses: zhangjz@lzu.edu.cn (J. Zhang), zhang_yiping@haust.edu.cn (Y. Zhang).

https://doi.org/10.1016/j.foreco.2026.123602
Received 30 November 2025; Received in revised form 2 February 2026; Accepted 4 February 2026
0378-1127/© 2026 Elsevier B.V. All rights are reserved, including those for text and data mining, AI training, and similar technologies.

species-specific climate responses is essential for predicting how ecotones will reorganize under continued climate change.

Tree growth is highly plastic in response to changing environmental conditions (Deslauriers et al., 2017), yet it remains unclear how species from different distributional ranges—particularly northern versus southern populations within mesic ecotones—respond to ongoing climate change. Addressing these uncertainties through observations at the cellular scale offers the potential for a more mechanistic understanding of xylogenesis (wood formation) and its environmental controls (Fonti et al., 2010). Such insights carry far-reaching implications, influencing predictions of tree survival, shifts in species distributions, and the dynamics of the global carbon cycle (Fang et al., 2001; Pan et al., 2011).

Xylogenesis, resulting from the growth and differentiation of the vascular cambium (Deslauriers et al., 2017), is a major determinant of long-term carbon sequestration (Pan et al., 2011; Pugh et al., 2020). Xylogenesis is a dynamic and sensitive biological process influenced by both external environmental factors (such as temperature and water conditions) and endogenous factors (such as tree species, age, and size) (Deslauriers et al., 2017). Studies indicate that temperature and photoperiod are the primary factors for the onset and end of coniferous tree growth in the Northern Hemisphere (Huang et al., 2020; Mu et al., 2023; Rossi et al., 2016). However, uncertainties remain in how cambial activity and radial growth respond to climatic factors. For example, while long-term monitoring of radial growth in *Juniperus przewalskii* across altitudinal and latitudinal over the cold and arid northeastern Tibetan Plateau reveals that temperature plays a critical role in growth onset (Zhang et al., 2021; Zhang et al., 2018a), other studies highlight that early-season water availability also influences growth initiation in this species (Ren et al., 2018). Growth duration and rate are the two primary parameters that jointly determine radial growth (Rathgeber et al., 2011). In cool, moist regions, growth duration contributes more to radial growth than rate, making it possible that warming will be the primary driver enhancing growth duration and total growth (Rossi et al., 2014). Conversely, in arid regions, growth rates are the primary constraint to total growth. In these regions, warming or intensified drought may limit growth by negatively affecting growth rates (Ren et al., 2019; Zhang et al., 2018a). For example, in 2016 on the northeastern Tibetan Plateau, a 16-day dry spell likely halted cambial growth in *J. przewalskii*, but with subsequent warm, wet conditions, growth resumed and over 60 % of trees extended their growing season by about a month compared to the previous five years (Zhang et al., 2020). These findings highlight the remarkable resilience of trees to extreme, short-term weather events and the potentially idiosyncratic impact of climate change on tree growth and the terrestrial carbon cycle. However, current monitoring of cambial phenology and intra-seasonal dynamics has focused largely on conifers, while broadleaf species, which comprise 60 % of global forest area, remain underrepresented, particularly in studies comparing ecological types within forest ecotones.

An additional level to understanding radial growth is that cambial activity and growth responses to climate also vary by species or wood types (Rossi et al., 2008b; Wang et al., 2023), age (Rossi et al., 2008a; Zhang et al., 2023), and size or canopy positions (Liu et al., 2018; Rathgeber et al., 2011). Species with contrasting wood anatomies exhibit distinct physiological requirements, including differing reliance on hydraulic transport, which shape their adaptive strategies. Consequently, inter-annual ring-width variability differs among wood types. Ring-porous species, for example, grow more rapidly early in the season than diffuse-porous and coniferous species because they must produce new vessel conduits annually to supply water during leaf development (Chen et al., 2022; García-González et al., 2016). Such anatomical differences are mirrored in the timing of xylem formation in coexisting coniferous and deciduous species (García-Cervigón et al., 2017; Martinez del Castillo et al., 2016). For instance, ring-porous trees often initiate growth earlier, forming earlywood vessels to reduce hydraulic failure risk during summer droughts (Baas and Wheeler, 2011), whereas diffuse-porous species typically peak later (D'Orangeville et al., 2022). Despite these insights, major gaps remain in understanding how growth timing and structure, across wood types, species, and distribution patterns, respond to climatic shifts and intrinsic factors in mesic ecotone forests.

In this study, we investigated the intra-seasonal dynamics of cambial phenology and xylogenesis in six tree species located near the northern or southern margins of their ranges within the mid-Northeastern United States forest ecotone. Monitoring was conducted at 7–10-day intervals throughout the 2019 growing season and into early 2020, until COVID-19 restrictions curtailed fieldwork. We monitored three southern species—*Quercus alba* (White Oak), *Carya ovata* (Shagbark Hickory), and *Betula lenta* (Sweet Birch), and three northern species—*Betula papyrifera* (Paper Birch), *Picea rubens* (Red Spruce), and *Larix laricina* (Eastern Larch). These represented ring-porous (*Q. alba*), semi-ring-porous (*C. ovata*), diffuse-porous (*B. lenta* and *B. papyrifera*), and coniferous (*P. rubens* and *L. laricina*) anatomical types. We aimed to identify differences in growth timing and dynamics among species with contrasting wood anatomies and distribution patterns. Specifically, we hypothesized that: (i) growth timing and magnitude are species-specific and shaped by both anatomical type and distribution status (southern, northern); (ii) temperature is the primary driver of radial growth onset, regardless of species traits, particularly under the contrasting early-season climatic conditions of 2019 and 2020; and (iii) competition dynamics, including canopy positions, exert significant influence on growth timing and rates in high-density mesic ecotone forests.

2. Materials and methods

2.1. Study area

Our study was conducted in Harvard Forest, a mixed deciduous, broadleaf-dominated forest situated within the central ecotone of the northeastern United States (Fig. 1). The canopy is dominated by *Quercus rubra* (Northern red oak) and *Acer rubrum* (Red maple), with lesser representation from *Fagus grandifolia* (American beech), *Tsuga canadensis* (Eastern hemlock), *Pinus strobus* (Eastern white pine), and *Betula alleghaniensis* (Yellow birch). Harvard Forest lies near the northern range limits of *Quercus alba*, *Carya ovata*, and *Betula lenta*, and the southern limits of *Betula papyrifera*, *Picea rubens*, and *Larix laricina*. Among these species, *Q. alba* and *C. ovata* are ring-porous, producing large earlywood vessels, with *C. ovata* also exhibiting semi-ring-porous characteristics. *B. lenta* and *B. papyrifera* are diffuse-porous, forming uniformly small vessels throughout the growth ring. *P. rubens* and *L. laricina* are conifers, the former evergreen and the latter a deciduous conifer. Samples from *Q. alba, C. ovata, B. lenta*, and *B. papyrifera* trees came from the same dense upland forest. The sampled *L. laricina* trees lived in a glacial pothole with a relatively low-density forest while samples for *P. rubens* came from trees living in a dense mixed *Picea* swamp.

2.2. Climate conditions

Daily temperature and precipitation have been recorded at the Harvard Forest weather station since 1964 (Boose et al., 2025). Based on these records, the climate is classified as temperate continental, with mean annual precipitation of 1111.9 mm, evenly distributed throughout the year, and a mean annual temperature of 8.1 °C, characterized by warm summers (20.7 °C in July) and cold winters (−5.3 °C in January). From 1964–2024, both temperature and precipitation exhibited increasing trends. Relative to the long-term average, conditions were cooler and wetter in 2019 and warmer and drier in 2020, particularly from January to May (Figure S1, Table S1). The 2019 mean annual temperature (7.9 °C) was 1.3 °C lower than in 2020 (9.2 °C), while annual precipitation was 259.6 mm higher in 2019 (1366.2 mm) than in 2020 (1106.6 mm). From January to May, temperatures were 1.4 °C lower in 2019 than in 2020, despite slightly warmer conditions in April

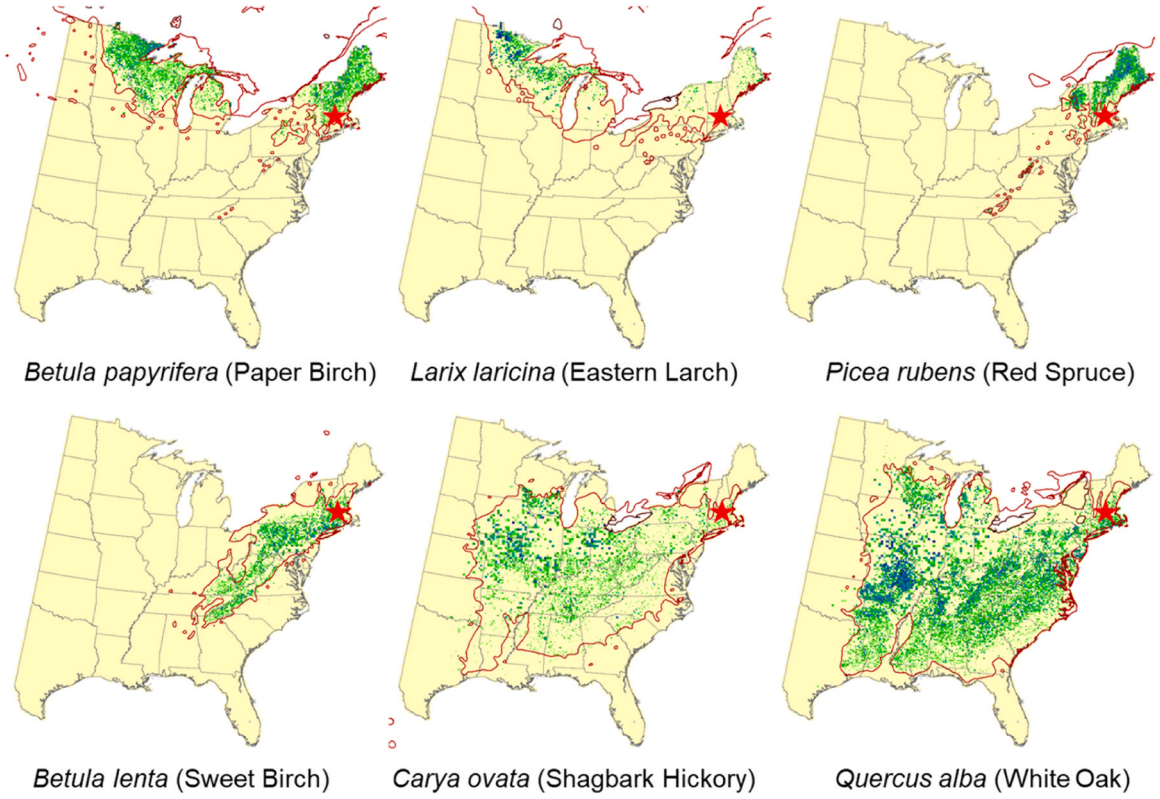

Fig. 1. Distribution of our study site (Harvard Forest, marked by red stars) and studied northern and southern species in eastern of United States. Tree species distribution data from Version 4 of the Climate Change Tree Atlas (https://www.fs.usda.gov/nrs/atlas/tree/).

2019.

2.3. Xylem sampling and preparation

Study trees were upright stems without reaction wood or visible damage to the lower bole. In 2019, we monitored 60 trees, ten individuals of each of six species. Seasonal wood development was tracked by extracting two microcores (2 mm diameter, 20 mm length) per tree using a Trephor (Rossi et al., 2006a) weekly from mid-April to late October. At the start of the 2019 growing season, we recorded diameter at breast height (DBH) and assigned each tree to one of four canopy classes: dominant, co-dominant, intermediate, or suppressed. Leaf development was noted at each visit until full expansion. In 2020, COVID-19 restrictions reduced the sample size to 36 trees. Sampling frequency was adjusted to one microcore per tree at 10-day intervals from 11 March to 25 June, resulting in no data for the late-season growth period.

Microcores were extracted along a spiral trajectory at breast height (1.3 m). Consecutive sampling points were spaced 3 cm apart to avoid intersecting resin ducts from adjacent cores. Immediately after collection, samples were fixed in a formalin–alcohol–acetic acid solution (5:90:5, v/v/v). In the laboratory, microcores were softened in glycerol, dehydrated through a graded ethanol series (70 %, 85 %, 95 %, and 100 %), cleared in xylene, and embedded in paraffin (Zhang et al., 2013). Transverse sections (12 μm thick) were cut with a rotary microtome (RM 2245, Leica, Germany), stained with 1 % safranin in water and 0.5 % fast green in 95 % ethanol, and examined under an optical microscope. Images were captured and analyzed using ImageJ software (Abràmoff et al., 2004).

Cambial activity and wood formation were assessed following the methods described by Zhang et al. (2021). For each microcore image, three radial files were selected to count cambial cells and to measure the widths of the three developmental phases: cell enlargement, cell-wall thickening, and maturation. Total ring width was calculated as the sum of these three phase widths. For the four hardwood species, we also counted vessels and measured their diameters and cross-sectional areas. In the ring-porous species (*Q. alba*) and the semi-ring-porous species (*C. ovata*), vessel counts and measurements were performed separately for earlywood and latewood, in addition to the total ring vessel analysis (Figure S2).

Cambial phenology was determined by identifying the day of the year (DOY) corresponding to the sampling dates of images showing: (i) onset of cell enlargement, (ii) onset of cell wall thickening, (iii) onset of cell maturation, (iv) end of cell enlargement, and (v) end of cell wall lignification. The duration of cell production was defined as the period between the onset and end of cell enlargement, whereas the duration of xylogenesis was defined as the period from the onset of cell enlargement to the end of cell wall lignification (Gruber et al., 2009).The width of xylem cells was standardized relative to the total width of the previous growth ring using the equation:

$$nc_{i=} nm_{i*} rw_m / rw_s$$

where nc_i is the standardized width of xylem cells, nm_i is the measured width of xylem cells, rw_m is the mean ring width of previous rings of all samples each tree, and rw_s is the ring width of previous rings for each sample.

2.4. Foliage phenology

Bud and leaf characteristics were recorded from April to June 2019 on the same trees used for wood sampling, except for *P. rubens*, the evergreen conifer. From these observations, we interpolated the timing of bud break and leaf development for each tree. Budburst was defined as the stage when $\geq$ 50 % of an individual's buds had emergent leaves, and leaf development as the stage when $\geq$ 75 % of leaves had reached 75 % of their mature size. Autumn leaf abscission data for *Q. alba, B.*

lenta, and B. papyrifera in 2019 were obtained from Harvard Forest tagged understory and overstory individuals located within 1.5 km of the study plots (Richardson and O'Keefe, 2009).

2.5. Statistical analysis

The increase in the total width of xylem cells was modeled using a Gompertz function in R (version 4.5.0, R Core Team, 2022):

$$Y = Ae^{-e^{(\beta-\kappa t)}}$$

where Y represents the cumulative width of xylem cells, t is the time expressed as DOY, A is the upper asymptote, associating to the final width of radial growth. β is the x-axis placement parameter and κ is the rate of change parameter. The date of perk growth rate (t_p) was calculated as β/κ and the corresponding maximum growth rate (R_{max}) was computed as $\kappa A/e$ (Rathgeber et al., 2011). The average growth rate (R_{mean}) was obtained by dividing total growth by the duration of cell production. Because the DBH of northern species was generally smaller than that of southern species (Table 1), total growth and R_{mean} were expressed relative to DBH, calculated as the ratio of total growth or growth rate to DBH, to remove size effects.

Analysis of variance (ANOVA) was used to compare timing, duration, growth rate, and total growth width among species and years, with Tukey's test applied for homogeneous variances and the Games–Howell test for heterogeneous variances. All variables were tested for normality and homogeneity of variance prior to ANOVA (Quinn and Keough, 2002). To examine the effects of DBH, species (*Q. alba*, *C. ovata*, *B. lenta*, *B. papyrifera*, *P. rubens*, and *L. laricina*), wood type (ring-porous, diffuse-porous, non-porous), distribution status (southern, northern), canopy position (dominant, co-dominant, intermediate, suppressed), tree taxa (angiosperm, conifer), and leaf habits (deciduous, evergreen) on cambial phenology and radial growth dynamics in 2019, we fitted linear mixed-effects models:

$$Y \sim \alpha + \beta DBH + a + b + c + d + e + f + \varepsilon$$

where Y is the dependent variables (Cambial phenology and growth parameters), DBH as a fixed effect, and species, wood type, distribution status, and canopy position as random effects. α is the intercept; β is the slope; a, b, c, d, e, and f are the random effect of the species, wood type, distribution status, canopy position, tree taxa, and leaf habits respectively; and ε is the error term. Because the onset of cell enlargement, wall thickening, and maturation was recorded in early 2020, mean January–May temperature was included as an additional fixed effect to assess temperature influence on phenology onset:

$$Y \sim \alpha + \beta_1 T + \beta_2 DBH + a + b + c + d + e + f + \varepsilon$$

where Y is the dependent variables (onset of cell enlargement, wall thickening, and maturation), *DBH* and January–May temperature (T) as a fixed effect. β_1–β_2 are the slopes. Interaction terms among fixed effects with variance inflation factors (VIF) > 5 were excluded to avoid multicollinearity. Marginal R^2 (fixed effects) and conditional R^2 (fixed + random effects) were calculated for each model. Linear mixed-effects models were performed using the R package "lme4" (Bates et al., 2015). All analyses and plots were constructed using the R statistical software (version 4.1.2, R Core Team, 2022).

Table 1
Characteristics of monitoring trees. DBH (diameter at breast height) represents as Mean ± one standard error.

Species	Distribution status	Wood type	DBH (cm)
Quercus alba (White Oak)	Southern	Ring-porous	35.8 ± 3.5
Carya ovata (Shagbark Hickory)	Southern	Semi-ring-porous	33.9 ± 3.4
Betula lenta (Sweet Birch)	Southern	Diffuse-porous	26.4 ± 1.0
Betula papyrifera (Paper Birch)	Northern	Diffuse-porous	23.6 ± 4.8
Picea rubens (Red Spruce)	Northern	Non-porous (conifer)	21.4 ± 1.7
Larix laricina (Eastern Larch)	Northern	Non-porous (conifer)	13.7 ± 1.2

3. Results

3.1. Intra-annual wood dynamics

Intra-annual radial growth dynamics varied markedly among species (Fig. 2). Southern species (*Q. alba*, *C. ovata*, and *B. lenta*) maintained more cambial cells and achieved greater radial growth than northern species (*B. papyrifera*, *P. rubens*, and *L. laricina*). In southern species, the number of cambial cells numbers ranged from 5 to 7 cells in dormancy to 6–9 during peak activity. In northern species, dormancy counts were 3–5 cells, reaching a maximum of six cells in the active phase.

During the growing season, widths of cells in the enlarging and wall-thickening phases followed bell-shaped curves, whereas maturing cell widths increased steadily to a plateau. Southern species generally had greater widths of enlarging and thickening cells than northern species, which resulted in wider annual rings. *Q. alba*, with its early growth onset, began forming enlarging cells in late April, reaching a maximum of 98.1 μm three weeks later (DOY 141) before declining. Wall thickening in *Q. alba* began one week after enlargement started but closely mirrored the enlarging cells by peaking on DOY 141 and then decreasing. Cell enlargement in the other five species began later than in *Q. alba*. Among all species, *C. ovata*, ultimately producing the widest rings, attained the largest widths of enlarging and thickening cells despite an intermediate season length. Enlargement in *C. ovata* peaked in mid-June (DOY 168), while thickening peaked about two weeks later (DOY 182) and continued until late September. The diffuse-porous *Betula* showed similar patterns as in *C. ovata*. Enlargement peaked in mid-June (DOY 168) and thickening in early July (DOY 189). Importantly, the southern *B. lenta* produced more cells and wider rings than *B. papyrifera*. *Picea rubens,* an evergreen conifer species, initiated enlargement on DOY 158 and thickening on DOY 167. Like *C. ovata*, *P. rubens* continued to cell maturation until late September. In contrast, the deciduous conifer *L. laricina* ceased growth the earliest among all species, DOY 200, despite initiating enlargement earlier than the birches. *L. laricina* had the lowest growth rates and produced the fewest cells, resulting in the narrowest rings in our study.

3.2. Cambial phenology and foliage phenology

Cambial and foliage phenology varied substantially among species and between years (Fig. 3, Table S2-S3). Overall, ring-porous species—most notably *Q. alba*—initiated growth earlier than species with other wood structures. Enlargement of *Q. alba* began in late April (DOY 118 in 2019; DOY 121 in 2020), 27–47 days ahead of other species in 2019. Early enlargement of *Q. alba* was again the earliest in 2020 when it began 22–27 days ahead of the other species. Cell-wall thickening of *Q. alba* commenced 19–38 days earlier in 2019 and 15–24 days earlier in 2020, while maturation began 22–41 days earlier in 2019 and 21–26 days earlier in 2020. In 2019, diffuse-porous species had the latest onset across all phases, though timing did not differ significantly from conifers (ANOVA, $p > 0.05$). Putting *Q. alba* aside, growth onset among the remaining five species in 2020 was not significantly different (ANOVA, $p > 0.05$). For the four non-ring-porous species, growth onset in 2019 was significantly later than in 2020 (ANOVA, $p < 0.05$)—by 11 days in *L. laricina*, 16 days in *P. rubens*, and 19 days in both *B. lenta* and *B. papyrifera* (Table S3).

In 2019, *L. laricina* completed cell enlargement (DOY 200) and maturation (DOY 227) earlier than any other species, making the species

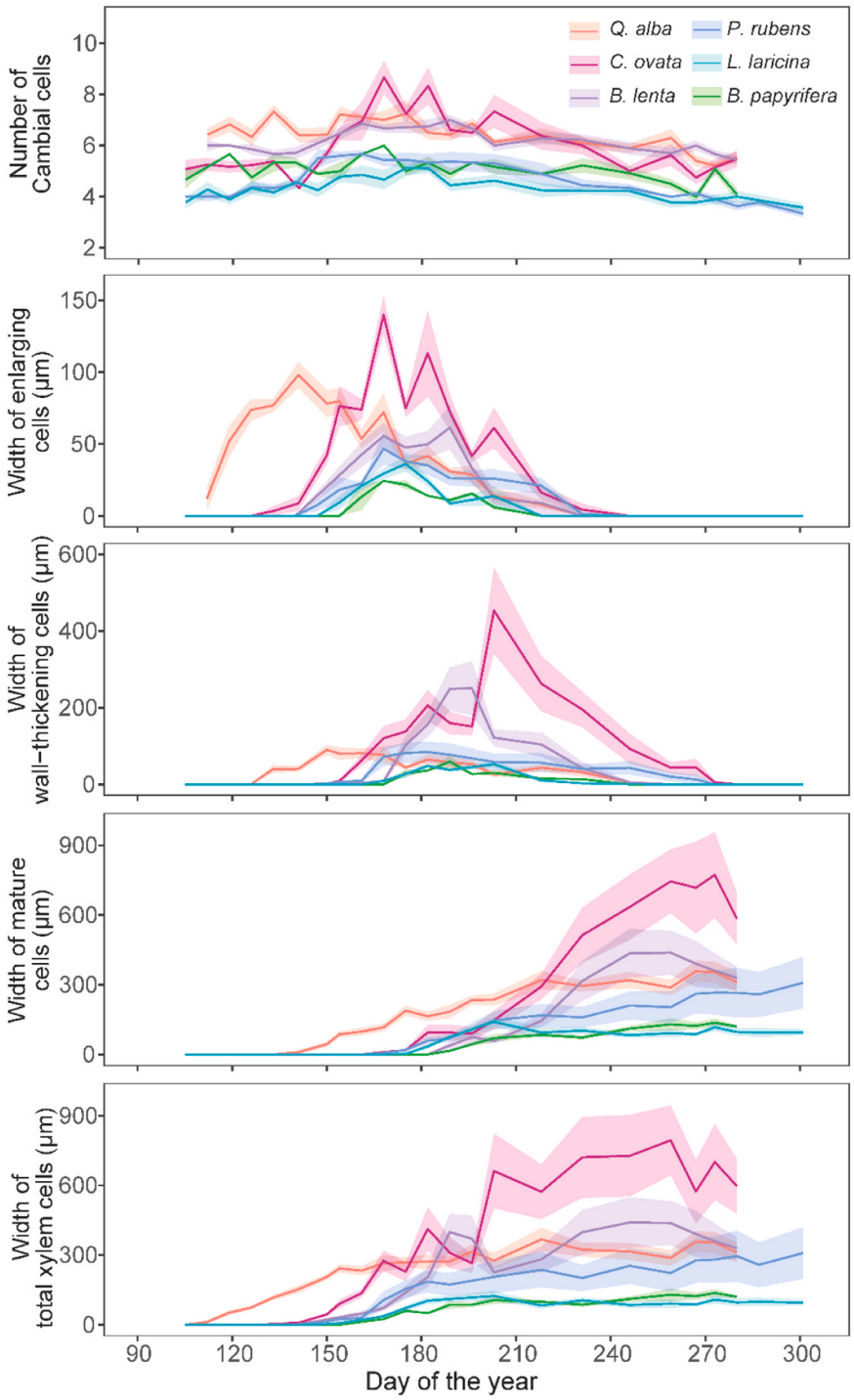

Fig. 2. The number of cambial cells and the width of radial growth during different developmental stages of xylogenesis in the six tree species throughout the 2019 growing season. Warm colors represent southern species, and cool colors represent more northern species. Shading represents the mean ± one standard error.

with the earliest end to the growing season (Fig. 3 and Table S2). Among the remaining species, cessation of cell division occurred in August (DOY 218–231) with no significant differences among them. The growing season ended for *Q. alba* and the diffuse-porous birches (*B. lenta*, *B. papyrifera*) in late August to early September (DOY 242–248), whereas *C. ovata* and *P. rubens* showed the latest cessation, in late September (DOY 263–268).

Because of its late onset and early termination, *L. laricina* had the shortest cell-production period—just 42 days (Fig. 3 and Table S2). The two *Betula* species also exhibited brief durations, each lasting 55 days. *C. ovata* and *P. rubens* were intermediate at 74 and 88 days, respectively. By contrast, the very early start of *Q. alba* yielded the longest cell-division period at 106 days. Growing-season length followed a similar pattern: *L. laricina* (69 days) and the birches (*B. lenta* 79 days; *B. papyrifera* 83 days) were shortest, *P. rubens* was intermediate (105 days), and the ring-porous *Q. alba* and *C. ovata* were longest (132 and 124 days, respectively).

Specifically, radial cell enlargement in *Q. alba* began 20 days before budburst in 2019, preceding both budburst and leaf expansion. In the remaining four species (*P. rubens* not measured), budburst occurred before cell enlargement. For *C. ovata*, budburst began 12 days earlier than enlargement, while 75 % leaf expansion occurred about five days

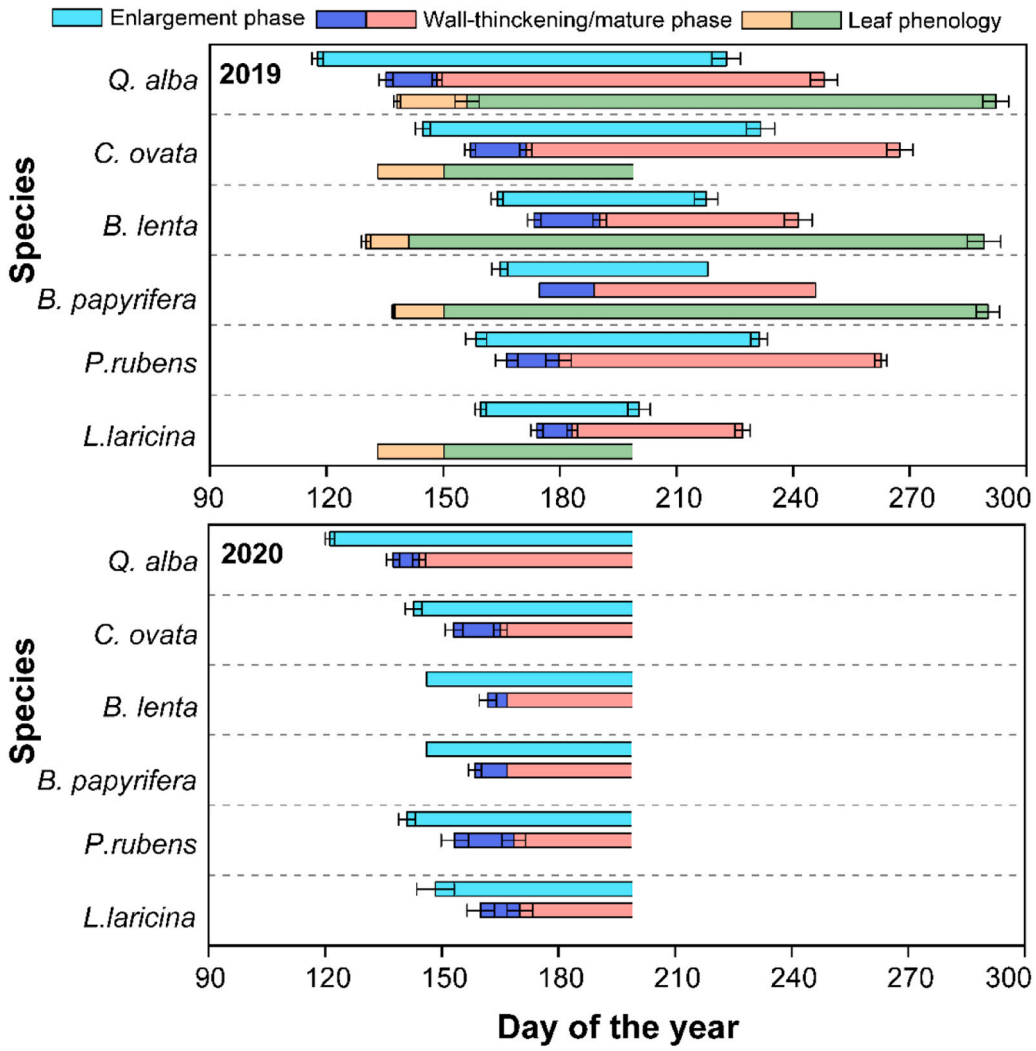

Fig. 3. Cambial and leaf phenology of different tree species during the 2019 and 2020 growing seasons. The beginning and end of the light blue horizontal bars indicate the timing of onset and cessation of cell enlargement, respectively. The beginning of the dark blue horizontal bars indicates the onset of wall-thickening, and the beginning and end of the red horizontal bars indicate the onset and end of cell maturation, respectively. The beginning of the yellow horizontal bars indicates the onset of bud burst, and the beginning and end of the green horizontal bars indicate 75 % leaf expansion and leaf abscission, respectively. Open bars indicate that no related phenology has been observed. Error bars represent the mean ± one standard error.

after enlargement onset. In *B. lenta*, *B. papyrifera*, and *L. laricina*, both budburst and 75 % leaf expansion occurred well before enlargement—budburst by 27–34 days and leaf expansion by 10–23 days. Leaf-abscission dynamics were only recorded for three species, *Q. alba*, *B. lenta*, and *B. papyrifera*. For these species, leaves were shed well after cambial activity ended—69–72 days after cell enlargement ceased and 44–47 days after cell maturation—without significant differences among species. While we do not have precise timing of *C. ovata* leaf

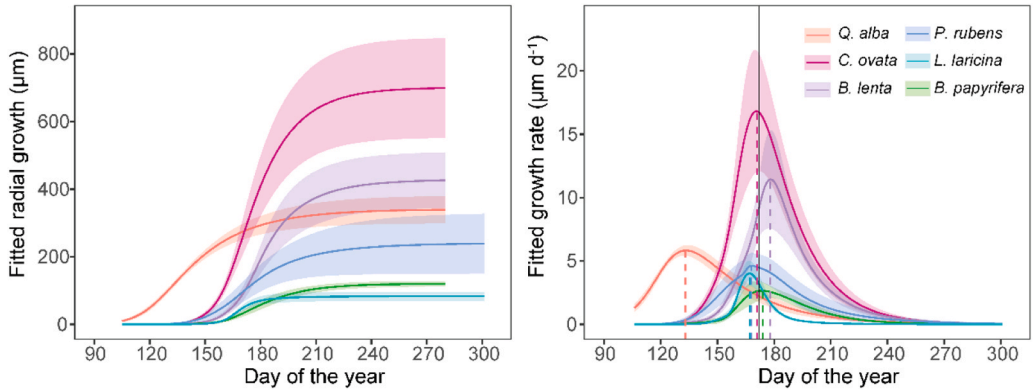

Fig. 4. Fitted radial growth and daily growth rate. Dashed lines indicate the dates of maximum growth rates among the species, while the black line marks the summer solstice in 2019 (DOY 172). Warm colors represent southern species, and cool colors represent more northern species.

abscission, it was observed to maintain leaves well after cambial activity ended.

3.3. Wood formation and growth rate

The Gompertz function effectively described total radial growth for all species, with goodness-of-fit values of 75–99 % (Fig. 4 and Table S2). Fitted results revealed marked interspecific differences in both total growth and growth rates (Fig. 4 and Fig. 5). Southern species showed substantially greater values than northern species: *C. ovata* attained the highest total growth (700.1 μm), 7.6 times that of *L. laricina* (92.1 μm), and its maximum growth rate (17.8 μm d^{-1}) was 6.8 times that of *B. papyrifera* (2.6 μm d^{-1}). Ring-porous species generally grew more than diffuse-porous and non-porous (conifer) species, with the latter exhibiting the lowest radial increments. Consistent with other phenological metrics, *Q. alba* reached its maximum growth rate in early May (DOY 133), more than a month before the other species. The remaining five species peaked between DOY 166–177, within a week of the summer solstice (DOY 172). Among these, diffuse-porous species peaked after the solstice, whereas ring-porous and non-porous species peaked beforehand.

Because northern species generally have smaller DBH than southern species (Table 1), we reduced the potential effect of DBH on growth and rate by expressing total growth and mean growth rate relative to each tree's DBH (Figure S3). Standardized totals for southern species remained higher than those of northern species, except for *Q. alba*, whose relative growth was lower than that of the northern *P. rubens*. Notably, *C. ovata* and *B. lenta* maintained higher relative mean rates than all northern species, whereas *Q. alba* had the lowest standardized mean rate among the six species.

3.4. Dynamics of vessels formation

In 2019, *Q. alba* formed earlywood vessels in late April, whereas *C. ovata* did so in late May (Table S2; Fig. 6). In both ring-porous species, vessel formation began within one week of fiber-cell enlargement onset. Despite this timing difference, earlywood vessel number, diameter, and area did not differ significantly between species: each averaged one vessel in 2019, with mean diameters of 181.2 μm (*Q. alba*) and 193.4 μm (*C. ovata*), and mean areas of 29,529 μm^2 and 27,836 μm^2, respectively. Latewood vessel formation was synchronous—early July (DOY 182 for *Q. alba*, DOY 189 for *C. ovata*)—but vessel size differed markedly. While both species produced a similar mean number (2.0 vs. 1.5), *C. ovata*'s vessels were substantially larger: total and mean diameters of 87.3 μm and 43.7 μm versus 32.8 μm and 21.9 μm for *Q. alba*. Total and mean areas were likewise greater in *C. ovata* (4 538.3 μm^2 and 2 269.2 μm^2) than in *Q. alba* (1 194.9 μm^2 and 796.6 μm^2).

Across the four hardwood broadleaf species, vessel number did not differ significantly (ANOVA, $p > 0.05$), although *B. papyrifera* averaged only 1.5 vessels compared with 2.3–2.9 in the other species despite living in the same watershed forest. In contrast, vessel size and area varied markedly. As expected, the large earlywood vessels of the two ring-porous species (*Q. alba*, *C. ovata*) resulted in significantly greater diameters and areas than those of the diffuse-porous species (ANOVA, $p < 0.05$). Among the two diffuse-porous species (*B. lenta* and *B. papyrifera*), vessel diameters and areas showed no significant variation across the growth ring, and vessel number, diameter, and area did not differ significantly between species (ANOVA, $p > 0.05$). However, total vessel area in *B. lenta* (8 410 μm^2) was roughly three times greater than in *B. papyrifera* (2 744 μm^2).

3.5. Impacts of climate and other factors on xylogenesis

Linear mixed-effects models showed that DBH had little influence on the onset of radial growth in 2019 (Table 2). A slight DBH effect was detected for the onset of the cell-wall-thickening phase, but only when climate impacts on growth phenology and dynamics were excluded. Model outputs revealed a substantial gap between marginal and conditional R^2, and higher standard deviations for species and wood type, indicating that these random factors contributed significantly to radial growth. In contrast, distribution status, canopy position, tree taxa, and leaf habits had no detectable effect on the onset of any growth phase. However, DBH played a larger role in determining the end of radial growth and overall growth duration. Larger trees ceased cell division and wall thickening later than smaller trees, resulting in longer growing seasons for larger trees (Figure S4). Among random factors, species exerted a strong influence on growth cessation, with *C. ovata* and *P. rubens* ending later and *L. laricina* ending earlier, a result that mirroring

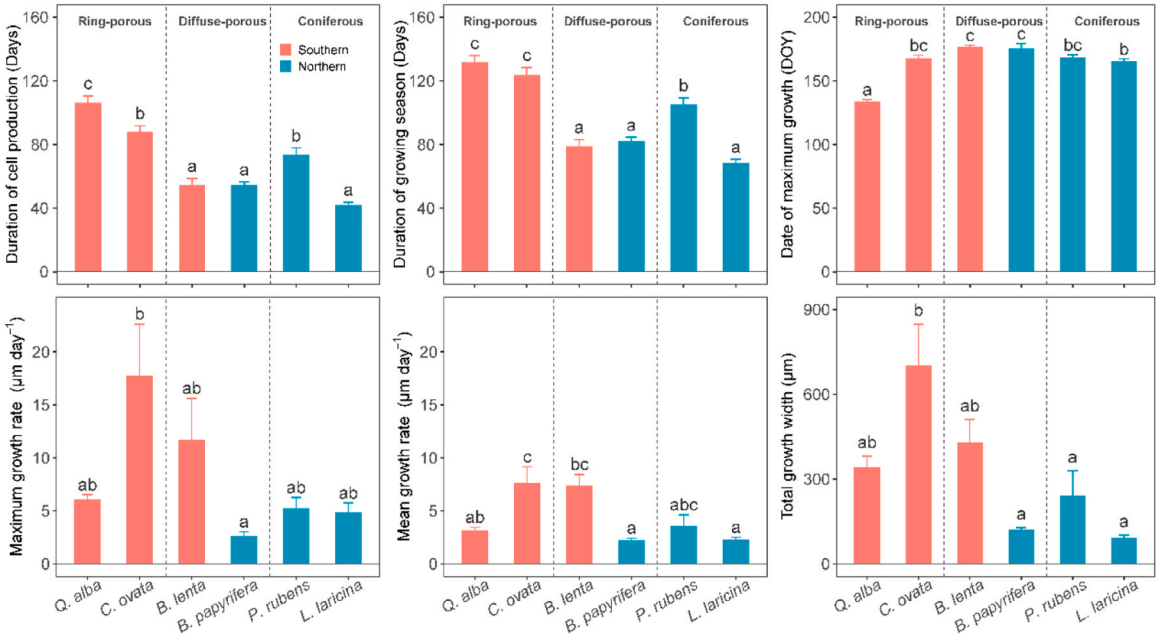

Fig. 5. Growth dynamics in different tree species. Values with the same letters above the bars are not significantly different at the 0.05 probability level (Tukey test). Error bars represent the mean ± one standard error.

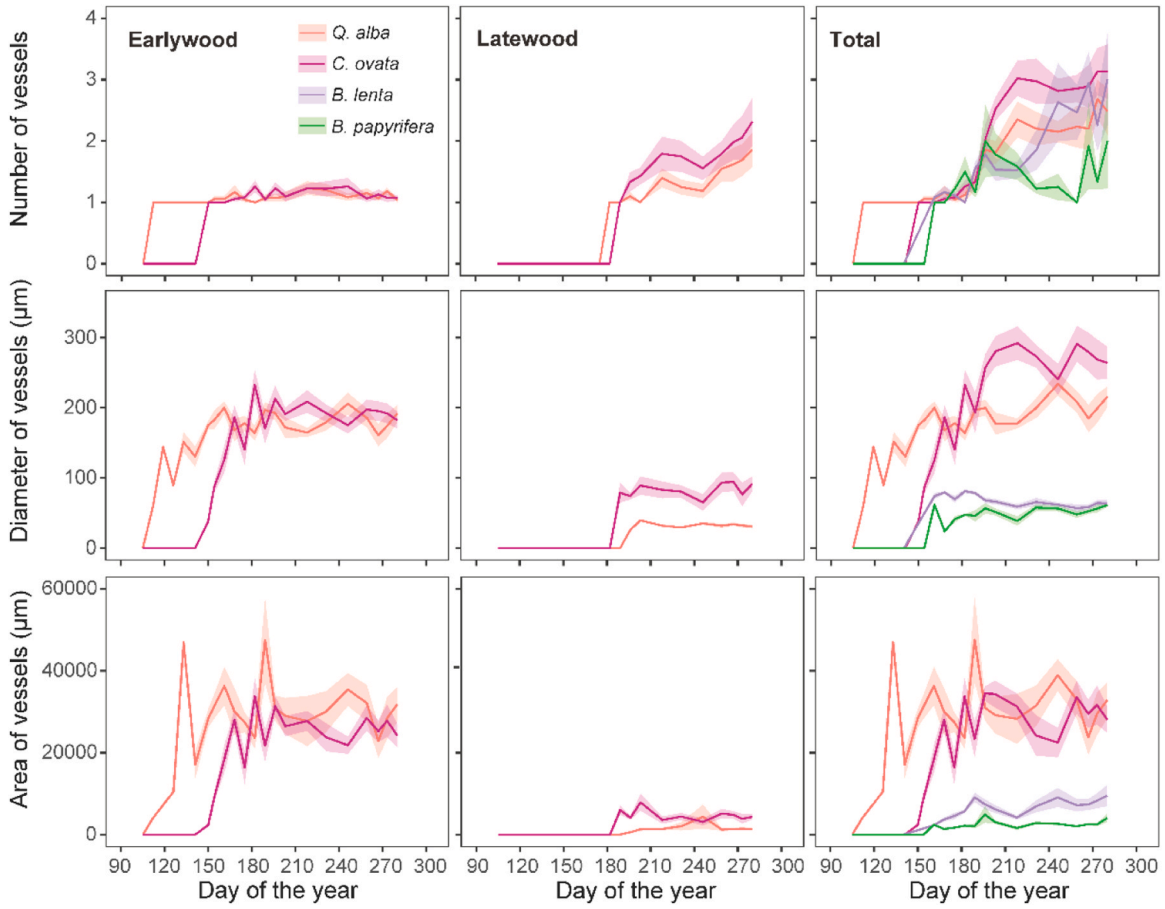

Fig. 6. The number, diameter, and area of vessels in the radial direction of four hardwood species throughout the 2019 growing season. Vessel dynamics in earlywood and latewood are also presented for the two ring-porous species (*Q. alba* and *C. ovata*). Shading represents the mean ± one standard error.

Table 2
Mixed-effect models for growth parameters and DBH during 2019. DBH is fixed effect and species, wood type, distribution status, canopy position, tree taxa, and leaf habits are random effects. Note: For fixed effects, estimate and its SE (in brackets) are given; $P < 0.001$ (***); $P < 0.01$(**); $P < 0.05$ (*); For random effects, SD of variances are given; Marginal R^2 (fixed effects only), Conditional R^2 (both fixed and random effects) are also provided.

	Fixed effects (estimate and SE)		Random effects (SD)							Model fit	
	Intercept	DBH	Species	Wood type	Distribution status	Canopy position	Tree taxa	Leaf habits	residual	Marginal R^2	Conditional R^2
OE	156.7 (9.8)**	-0.2 (0.1)	10.8	14.4	0.0	0.0	0.0	0.0	5.6	0.01	0.91
OT	172.1 (8.0)***	-0.3 (0.1)**	8.7	11.3	0.0	0.0	0.0	0.0	5.6	0.05	0.87
OM	183.0 (8.6)***	-0.2 (0.1)	9.1	12.3	0.0	0.0	0.0	0.0	6.0	0.02	0.87
EE	212.0 (14.0)*	0.5 (0.2)**	4.5	0.0	0.0	1.5	7.9	8.9	8.9	0.06	0.83
EL	237.7 (10.6)*	0.5 (0.2)**	11.1	0.0	0.0	3.2	0.0	11.3	7.8	0.08	0.83
DP	56.7 (17.4)	0.7 (0.2)**	8.4	20.1	0.0	2.8	0.0	14.6	10.8	0.06	0.87
GS	86.9 (21.8)*	0.7 (0.2)**	1.9	24.4	0.0	4.0	0.0	21.5	10.8	0.05	0.91
tp	163.6 (7.8)***	-0.1 (0.1)	13.7	6.0	0.0	5.4	0.0	0.0	5.6	0.00	0.89
W	-65.9 (150.8)	13.2 (4.4)**	136.3	0.0	83.8	104.2	0.0	0.0	236.4	0.18	0.50
R_{max}	-1.2 (4.2)	0.4 (0.1)*	4.0	0.0	0.0	1.4	0.0	0.0	8.3	0.14	0.32
R_m	1.0 (1.8)	0.1 (0.1)*	1.9	0.0	1.1	1.2	0.0	0.0	2.6	0.09	0.54
nV	0.9 (0.7)	0.04 (0.02)*	0.26	0.0	0.50	0.37			0.90	0.10	0.43
dV	59.4 (91.8)	2.2 (0.9)*	39.6	118.5	0.0	33.1			37.3	0.02	0.92
aV	3538 (13090)	301.6 (172.4)	0.0	16077	2871	6272			7352	0.02	0.85

OE/OT/OM: Onset of cell enlarging/wall-thickening/mature cell (DOY); EE/EL: End of cell enlargement/wall lignification (DOY); DP/GS: Duration of cell production/growing season (days); W: width of ring formation (μm); Rmax/Rm: Maximum/mean growth rate (μm/d); tp: Timing of maximum growth rate occurred (DOY); nV/dV/aV: Number/diameter/area of total vessels.

the role of species in the timing of onset timing. Unlike onset, wood type had no effect on the end of growth, whereas canopy position and leaf habits contributed significantly. Consequently, species influencing both onset and end, wood types affecting onset, and canopy positions and leaf

habits influencing cessation all shaped growth duration. These same factors strongly affected the timing of maximum growth rate, while distribution status had no measurable phenological effect. DBH also significantly affected total radial growth and growth rate: larger trees exhibited higher rates and greater cumulative growth. Species, distribution status, and canopy position all influenced growth and growth rate, whereas wood type did not. Specifically, southern tree species exhibited significantly greater growth rates than northern species, and dominant and co-dominant trees showed markedly higher growth rate compared to intermediate and suppressed trees. DBH had only slight effects on vessel number and diameter and did not influence vessel area. Vessel number was affected by species, canopy position, and distribution status, with southern tree species (especially *C. ovata*) and dominant trees exhibiting a higher vessel number. In contrast, vessel diameter and area were more strongly associated with wood type, as ring-porous wood had significantly larger vessels than diffuse-porous wood.

In 2020, expanded onset data coupled with contrasting climatic conditions allowed assessment of climate influences on growth phenology (Table 3; Figure 7, S5–S6). Warmer late-winter and early-spring temperatures advanced growth onset significantly ($p < 0.001$). Aside from temperature, the factors affecting radial-growth onset were consistent across both years: species identity and wood type contributed significantly, whereas DBH, distribution type, canopy position, tree taxa, and leaf habits had no detectable effect.

4. Discussion

While our study revealed how these multiple factors drove processes of xylem formation or interacted with one another through these processes, evidence suggests there might be important differences in overall growth rates between more northerly and southerly species growing in the same ecotone. However, no differences were observed in the timing of growth between these two broad taxonomic groups—a finding that does not support our first hypothesis. Specifically, southern species generally had greater growth rates, with the exception for *Q. alba* when we relativized growth based on DBH. Much more work is required to know if these results are consistent across populations. For now, our work lays a foundation for developing and testing hypotheses between more southerly and northerly tree species growing within the same region in terms of stem phenology and productivity. Tree size and species appeared to have an important influence on the duration of growth. Overall, our limited study indicated potential gains in understanding when studying a wide range of tree species, tree sizes, wood type, and canopy classes from nearly opposing geographic species within the larger geographic ecotone.

4.1. Growth peak between different wood types

We found that all species except *Q. alba* reached peak growth near the summer solstice, when day length is longest; *Q. alba* peaked nearly a month earlier (mid-May; DOY 134). This pattern aligns with previous Northern Hemisphere studies suggesting that photoperiod-regulated processes may enable trees to complete growth within a limited season and prepare for winter (Huang et al., 2014; Rossi et al., 2006b). Mixed-effects models indicated that, except for species identity, canopy position significantly influenced peak timing—consistent with light being a key regulator of tree biological clocks—as reflected in position-related shifts in our dataset (Huang et al., 2020).

While peak cambial growth timing showed some consistent patterns, we also observed clear differences linked to wood type. For example, despite being distributionally contrasting species, the two diffuse-porous, *B. lenta* and *B. papyrifera*, showed peak growth later than the others and not long after the summer solstice. This finding supports a six-year dendroband study of 610 trees spanning multiple wood types in the same larger research forest, which reported diffuse-porous species achieving maximum rates significantly later than others (D'Orangeville et al., 2022). We refined the estimated timing of diffuse-porous species' peak growth because prior dendroband studies, while relatively frequent, relied on inconsistent cambial growth observations. In contrast, our microcoring approach provided regular, temporally precise measurements—though only over a single year. Expanding such work across multiple years and a broader range of species will be essential to more accurately identify both the timing and the underlying drivers of mid-season cambial growth, whether governed by photoperiod, hydroclimate, canopy position, temperature, or a combination of these and other factors.

4.2. Impacts of temperature on the onset of xylogenesis

Our two-year monitoring of early-season growth captured interannual variation in the onset of intra-annual radial growth under contrasting climatic conditions. In 2020, a warmer year, radial growth began significantly earlier than in 2019 in five of six study species, underscoring the dominant influence of temperature on growth initiation. *Q. alba*, the most distinctly ring-porous species examined, showed no difference in onset timing between years. These findings support our second hypothesis and align with extensive evidence of temperature's pivotal role in initiating tree growth across the Northern Hemisphere (Huang et al., 2020; Rossi et al., 2016), whether in humid pure forests (Rossi et al., 2014), the mesic Harvard Forest in the northeastern U.S., or arid regions such as the northeastern Tibetan Plateau (Zhang et al., 2018b; Zhang et al., 2023). This finding is also in line with many studies that report the importance of temperature to the onset of xylogenesis in experimental conditions (Gričar et al., 2006; Oribe et al., 2003; Rademacher et al., 2022). While some studies report that pre-season precipitation can strongly influence onset in arid regions (Ren et al., 2018; Ziaco et al., 2018), our findings reinforce the consensus that temperature is the principal control in cooler climates, even under varying water availability. In fact, the onset of xylogenesis occurred 15-days later during the wet but cooler spring of 2019 versus the relatively dry spring of 2020. However, the COVID-19 pandemic prevented us from completing the scheduled sampling in 2020. This limitation restricted

Table 3
Mixed-effect models for cambial phenology and temperature and DBH during 2019 and 2020. Temperature and DBH are fixed effects, species, wood type, distribution status, canopy position, tree taxa, and leaf habits are random effects. Note: For fixed effects, estimate and its SE (in brackets) are given; $P < 0.001$ (***); $P < 0.01$(**); $P < 0.05$ (*); For random effects, SD of variances are given; Marginal R^2 (fixed effects only), Conditional R^2 (both fixed and random effects) are also provided.

	Fixed effects (estimate and SE)			Random effects (SD)							Model fit	
	Intercept	Temperature	DBH	Species	Wood type	Distribution status	Canopy position	Tree taxa	Leaf habits	residual	Marginal R^2	Conditional R^2
OE	170.8 (8.7) ***	-11.6 (2.2) ***	-0.1 (0.1)	10.0	10.0	0.0	0.0	0.0	0.0	7.2	0.09	0.81
OT	181.1 (7.8) ***	-9.5 (2.0)***	-0.2 (0.1)	7.0	9.7	0.0	0.0	0.0	0.0	6.7	0.09	0.78
OM	199.1 (7.6) ***	-13.4 (1.8) ***	-0.1 (0.1)	8.7	8.9	0.0	0.0	0.0	0.0	6.1	0.15	0.84

OE/OT/OM: Onset of cell enlarging/wall-thickening/mature cell (DOY).

our capacity to compare the end growth phenology across species and to identify factors that govern the timing of growth cessation among different tree species. Furthermore, observed growth differences may reflect the relatively short duration of monitoring rather than genuine interspecific variation. Nonetheless, we have opted to present these data in their current form due to the scarcity of studies on several of the included species, particularly *B. lenta* and *C. ovata*, and the value of comparing co-occurring species with contrasting biogeographic affinities within the same forest (specifically, the more southerly distributed *B. lenta*, *C. ovata*, and *Q. alba* versus the more northerly *B. papyrifera*).

4.3. Impacts of DBH and canopy position on xylogenesis

Although we observed a strong correlation between diameter at breast height (DBH) and the timing of growth initiation in this mesic mixed forest, mixed-effects modeling indicated that DBH does not significantly influence the onset of radial growth. In contrast, both linear analyses and mixed-effects models revealed significant effects of DBH on growth cessation, duration, rate, and total growth. Larger trees tended to cease growth later, maintain longer growing seasons, exhibit higher growth rates, and achieve greater total growth than smaller trees. Consistent with these patterns, canopy position—closely linked to DBH in our dataset—also affected growth cessation, duration, rate, and total growth, but not the onset of growth. These results support our third hypothesis, namely that competition dynamics—including canopy position—significantly influence both the timing and rates of growth in high-density mesic ecotone forests. The influence of canopy position likely reflects competitive status rather than tree diameter per se, as larger trees generally occupied more advantageous canopy positions (Figure S7). This is consistent with previous reports for canopy-dominant conifers, which show later cessation of cambial activity, significantly longer growing seasons, and greater total growth than suppressed individuals (Liu et al., 2018; Rathgeber et al., 2011; Vieira et al., 2014). Our findings suggest that this relationship also applies to broadleaf species. In line with competition-related effects, forest thinning has been shown to extend growing seasons and enhance xylem production, with dominant trees sustaining longer periods of xylogenesis and producing more xylem (Grotta et al., 2005; Linares et al., 2009).

In our dense, mixed mesic forest, competition among trees influenced cambial phenology, indicating that light availability plays an important role in regulating tree-growth timing. The absence of a canopy-position effect on growth initiation may be explained by the lack of leaves early in the growing season in *Q. alba* and the sparse foliage of newly emerged leaves in the other five species—both phenologies allowing substantial light penetration to the forest floor. However, because radial growth cessation occurred roughly 50 days before leaf abscission (Fig. 3), it is reasonable to infer that shading from fully developed foliage reduces light availability to lower-canopy trees, resulting in earlier growth cessation and shorter growth duration.

Dominant trees, by capturing more sunlight, exhibit higher photosynthetic rates and carbohydrate fixation, supporting greater radial growth under otherwise similar conditions (Campoe et al., 2013). Tree competition may also influence growth and climate sensitivity, though its full impact remains unclear. Evidence suggests that growth in dominant or large trees is more temperature-sensitive than in suppressed individuals (Anderson-Teixeira et al., 2022; Liu et al., 2018), while understory trees may respond non-linearly and negatively to elevated temperatures (Rollinson et al., 2021). Trees with wider rings tend to be more vigorous and responsive to meteorological events than those with narrower rings, as reflected in intra-annual density fluctuations and episodic radial growth (Miller et al., 2022; Popkova et al., 2018; Rigling et al., 2001; Zhang et al., 2020). These dynamics often involve temporary pauses in cambial activity followed by reactivation, driven by short-term climatic shifts. For instance, droughts early in the growing season can produce cells typical of late-season conditions (Gao et al., 2021), while subsequent rainfall may trigger early-season cell formation (Zhang et al., 2020). Although further research is needed, our findings indicate that canopy status and stem diameter significantly influence late-season cambial dynamics and phenological patterns.

4.4. Relationship between foliage phenology and cambial phenology

By comparing leaf phenology and radial growth phenology, we found that the onset of radial growth in the ring-porous tree species *Q. alba* is significant earlier than budburst and leaf expansion. A similar pattern was observed in the semi-ring porous *Carya ovata*, where cambial activity precedes leaf unfolding. In contrast, diffuse-porous species (*B. lenta* and *B. papyrifera*) and the deciduous conifer *L. laricina* initiate radial growth well after budburst. Such patterns are further supported by findings from other species in Harvard Forest, where *Q. rubra* (ring-porous) initiates radial growth before budburst, in contrast to *A. rubrum* (diffuse-porous), which begins growth post-budburst (Chen et al., 2022). Such contrasts align with previous studies showing that in ring-porous species, xylem formation reliably precedes leaf development (Dox et al., 2022; Gricar et al., 2022). Our results reinforce the notion that leaf and cambial phenology are asynchronous, with their sequence varying across wood anatomical types—reflecting distinct ecological strategies and adaptive responses (Begum et al., 2013). Additionally, comparing the two conifer species, although we lack data on leaf phenology, we found that the growth cessation of *P. rubens*—the only evergreen species in this study, occurred more than one month later than that of the deciduous conifer *L. laricina*. This suggests that leaf habits (deciduous vs. evergreen) may also influence the timing of radial growth cessation.

Earlywood vessels in ring-porous species are critical for maintaining hydraulic function at the onset of the growing season, as they become nonfunctional after one year (Kitin and Funada, 2016; Kudo et al., 2018). These vessels facilitate water transport shortly after budburst, before current-year leaves fully expand, and are typically formed within a week of radial growth initiation (Fig. 6). While their large diameter enhances spring conductivity compared to diffuse-porous and nonporous species, it also increases vulnerability to cavitation under water-limited conditions (Baas and Wheeler, 2011). Ring-porous trees, exemplified by *Q. alba*, consistently initiate radial growth earlier than other wood types, with minimal interannual variation despite differing early-season temperatures (Fig. 7). This early onset likely compensates for hydraulic losses caused by late-summer droughts and winter freeze-thaw cycles (Sperry et al., 1994), suggesting that growth timing in ring-porous species is primarily genetically regulated. In contrast, conifer tracheids and diffuse-porous vessels, which are more resistant to embolism, reduce the need for early cambial reactivation (Hunter and Lechowicz, 1992; Sperry et al., 1994).

Budburst marks a critical transition, shifting the energy source for wood formation from stored carbon to carbon produced by new photosynthetic structures (Huang et al., 2014). In ring-porous species, without budburst or leaf development, radial growth initiation relies on carbohydrates stored from the previous year. For example, *Quercus pubescens* in the sub-Mediterranean show that leaf phenology significantly influences xylem phenology the following year, reflecting a "legacy response" (Gricar et al., 2022). In contrast, diffuse-porous species and *Larix* spp. initiate radial growth after leaf emergence, when newly formed leaves have already fixed sufficient carbon to support cambial activity. Their delayed growth onset allows conservation of stored reserves during leaf flush and aligns with their indeterminate shoot growth strategy (Barbaroux and Bréda, 2002).

4.5. Adaptability of Northern and Southern species

While cambial phenology varied among species, intriguingly, there were no significant differences between northern and southern taxa. In contrast, we observed marked variation in growth rate and radial

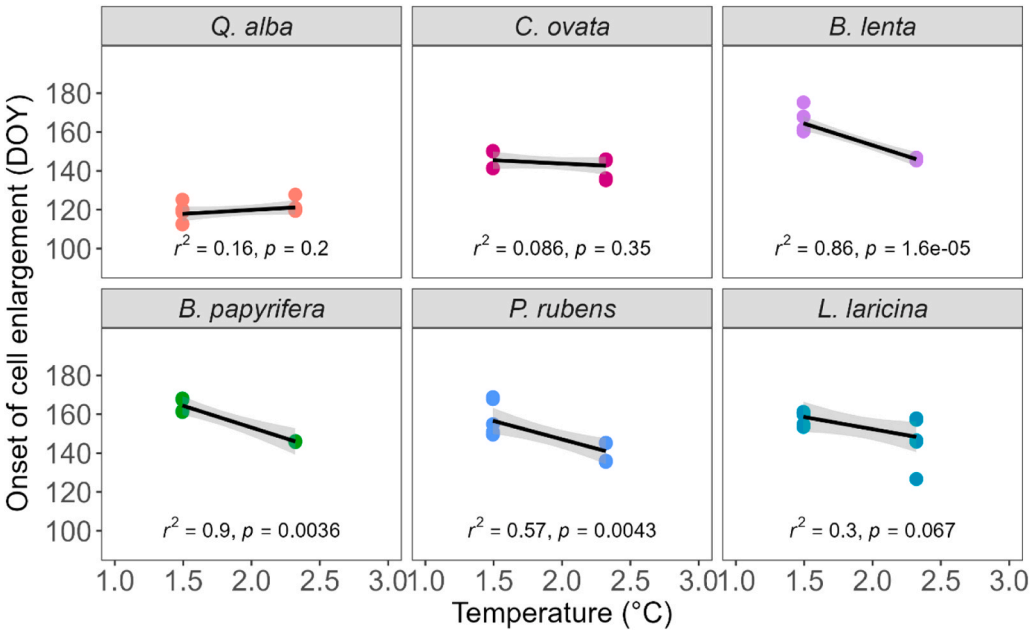

Fig. 7. Relationship between growth onset and temperature during 2019 and 2020 among different species.

growth increment. For instance, the more southern *B. lenta* and the more northern *B. papyrifera* exhibited comparable growing season lengths, yet *B. lenta* achieved approximately 3.6 times the growth increment of *B. papyrifera*. Even after accounting for DBH effects, the relative radial growth of *B. lenta* remained 2.9 times greater. These results point to potentially distinct growth strategies between northern and southern species, despite similarities in phenological timing.

We also found notable differences linked to species' geographic distributions. In southern species, growth rate appeared to be the primary driver of total wood production, while growth duration played a comparatively minor role—an extended growing season did not necessarily result in greater wood yield. In northern species, by contrast, both growth rate and growth duration contributed substantially to total growth (Figure S8). This pattern echoes findings from temperate arid and semi-arid regions, where the rate of cell production accounts for over 75 % of the variability in tree-ring width (Rathgeber et al., 2011; Ren et al., 2019; Zhang et al., 2021; Zhang et al., 2018a). In boreal forests, however, growth duration is even more critical, explaining 86 % of annual variability in wood productions surpassing the influence of rate (Rossi et al., 2014). Our results align with tendencies observed in species near the center of their ranges. Strikingly, these contrasting strategies emerged even among species concurring in the same broader landscape—or, for *Betula*, even within the same stand. This suggests that the traits underlying total wood production may be evolutionarily conserved. Overall, the differing contributions of growth rate and duration across environments underscore distinct radial growth strategies and the importance of geographic context in shaping wood production.

In southern temperate regions, adaptation to potential water deficits under warm and possibly drier conditions makes radial growth more sensitive to water availability than to temperature (Tyrgotov et al., 2024). Under relatively wet conditions, accelerated cambial activity and higher cell-division rates enable substantial cell production within a shorter time frame, helping trees mitigate the impacts of summer drought. Consistent with this, previous studies have shown that water availability is a key driver of tree-ring formation in these species (Fritts, 1962; Rudolph et al., 2024; Wagner et al., 2012; Wiles et al., 2025), including across the eastern United States in eight southern broadleaf species (Martin-Benito et al., 2015). By contrast, northern species adapted to colder, boreal climates are more strongly influenced by temperature than by water availability (Rossi et al., 2014). Warmer conditions extend the period of cambial activity, promoting xylem production through earlier growth initiation and delayed cessation (Rossi et al., 2016). Likewise, other studies have shown that temperature alone, or in combination with precipitation, significantly affects growth in these species (D'Orangeville et al., 2025; Sullivan et al., 2021).

5. Conclusion

Our study on the concurrent cambial phenology and growth dynamics of six tree species representing contrasting range distributions, and wood types within a regional ecotone found significant differences among species. Our inclusion of diffuse-porous and ring-porous broadleaf species, especially those whose distributions are from differing biomes, starts to fill an important gap in xylogenetic research. We found that ring-porous species initiate growth earlier than other wood types and show lower sensitivity to climate change. Overall, our research across a diverse set of species suggests distinct growth strategies. Although growth phenology between southern and northern species shows no significant differences, southern species exhibit higher growth rates and radial growth increments than northern species, even after eliminating the influence of DBH. We hypothesize that these groups might be adopting different growth strategies: southern species rely on water-limited adaptations, while northern species are more temperature-limited. Our findings, despite limited temporal coverage, provide novel insights and testable hypotheses to advance physiological and ecological models of tree-climate interactions and offer valuable insights into tree growth dynamics and distribution capacities under climate change. These results are therefore important for the management and conservation of mixed forests within ecotones. Although limited in scope, this work may also inform perspectives and stewardship strategies regarding more northerly and southerly tree species in similar forest systems.

CRediT authorship contribution statement

Keyan Jiang: Methodology, Formal analysis. **David Orwig:** Writing – review & editing. **Neil Pederson:** Writing – review & editing, Supervision, Project administration, Methodology, Investigation, Conceptualization. **Junzhou Zhang:** Writing – review & editing, Writing –

original draft, Visualization, Methodology, Formal analysis, Conceptualization. **Yiping Zhang:** Writing – review & editing, Visualization, Project administration, Methodology, Investigation. **Min Li:** Writing – review & editing, Visualization, Methodology, Formal analysis. **Junliang Xu:** Writing – review & editing, Methodology, Investigation. **Tessa Mandra:** Methodology, Investigation.

Declaration of Competing Interest

The authors declare that they have no known competing financial interests or personal relationships that could have appeared to influence the work reported in this paper.

Acknowledgements

The authors sincerely thank Jiayu Hou and Lexin Zhai for their generous assistance in preparing the paraffin sections of microcores. This work is supported by U.S. Dept. of Agriculture Joint Venture Agreement (No. 22-JV-11242306–078), NSF Foundation LTER-06 (No. DEB–1832210). Junzhou Zhang is supported by the National Natural Science Foundation of China (No. 42477482) and the China Scholarship Council (No. 202306180123). Yiping Zhang is supported by the National Natural Science Foundation of China (No. 42271057) and International Science and Technology Cooperation Projects of Henan Province (No. 262102521053).

Appendix A. Supporting information

Supplementary data associated with this article can be found in the online version at doi:10.1016/j.foreco.2026.123602.

Data availability

Data will be made available on request.

References

Abràmoff, M.D., Magalhães, P.J., Ram, S.J., 2004. Image processing with ImageJ. Biophotonics Int. 11 (7), 36–42.
Anderson-Teixeira, K.J., Herrmann, V., Rollinson, C.R., Gonzalez, B., Gonzalez-Akre, E. B., Pederson, N., Alexander, M.R., Allen, C.D., Alfaro-Sanchez, R., Awada, T., Baltzer, J.L., Baker, P.J., Birch, J.D., Bunyavejchewin, S., Cherubini, P., Davies, S.J., Dow, C., Helcoski, R., Kaspar, J., Lutz, J.A., Margolis, E.Q., Maxwell, J.T., McMahon, S.M., Piponiot, C., Russo, S.E., Samonil, P., Sniderhan, A.E., Tepley, A.J., Vasickova, I., Vlam, M., Zuidema, P.A., 2022. Joint effects of climate, tree size, and year on annual tree growth derived from tree-ring records of ten globally distributed forests. Glob. Chang Biol. 28 (1), 245–266.
Baas, P., Wheeler, E., 2011. Wood anatomy and climate change. Climate Change, Ecology and Systematics. Cambridge University Press, Cambridge (UK), pp. 141–155.
Barbaroux, C., Bréda, N., 2002. Contrasting distribution and seasonal dynamics of carbohydrate reserves in stem wood of adult ring-porous sessile oak and diffuse-porous beech trees. Tree Physiol. 22 (17), 1201–1210.
Bates, D., Mächler, M., Bolker, B., Walker, S., 2015. Fitting linear mixed-effects models Usinglme4. J. Stat. Softw. 67 (1).
Begum, S., Nakaba, S., Yamagishi, Y., Oribe, Y., Funada, R., 2013. Regulation of cambial activity in relation to environmental conditions: understanding the role of temperature in wood formation of trees. Physiol. Plant 147 (1), 46–54.
Boose, E., Gould, E., VanScoy, M., 2025. Harvard Forest Climate Data since 1964, Harvard Forest Data Archive: HF300 (v.13). Environmental Data Initiative.
Campoe, O.C., Stape, J.L., Nouvellon, Y., Laclau, J.-P., Bauerle, W.L., Binkley, D., Le Maire, G., 2013. Stem production, light absorption and light use efficiency between dominant and non-dominant trees of Eucalyptus grandis across a productivity gradient in Brazil. For. Ecol. Manag. 288, 14–20.
Charrier, G., Martin-StPaul, N., Damesin, C., Delpierre, N., Hänninen, H., Torres-Ruiz, J. M., Davi, H., 2021. Interaction of drought and frost in tree ecophysiology: rethinking the timing of risks. Ann. For. Sci. 78 (2).
Chen, Y., Rademacher, T., Fonti, P., Eckes-Shephard, A.H., LeMoine, J.M., Fonti, M.V., Richardson, A.D., Friend, A.D., 2022. Inter-annual and inter-species tree growth explained by phenology of xylogenesis. N. Phytol. 235 (3), 939–952.
D'Orangeville, L., Itter, M.S., Dos Santos, J.M., Taylor, A.R., 2025. Can tree-rings inform assisted migration? Revisiting provenance trials across Atlantic Canada to compare local adaptation between red spruce populations. For. Ecol. Manag. 578.
Deslauriers, A., Fonti, P., Rossi, S., Rathgeber, C., Gričar, J., 2017. Ecophysiology and Plasticity of Wood and Phloem Formation. In: AmorosoLori, M.M., Daniels, L.D., Baker, P.J., Camarero, J.J. (Eds.), Dendroecology, Tree-Ring Analyses Applied to Ecological Studies. Springer International Publishing, pp. 13–33.
D'Orangeville, L., Itter, M., Kneeshaw, D., Munger, J.W., Richardson, A.D., Dyer, J.M., Orwig, D.A., Pan, Y., Pederson, N., 2022. Peak radial growth of diffuse-porous species occurs during periods of lower water availability than for ring-porous and coniferous trees. Tree Physiol. 42 (2), 304–316.
Dox, I., Mariën, B., Zuccarini, P., Marchand, L.J., Prislan, P., Gričar, J., Flores, O., Gehrmann, F., Fonti, P., Lange, H., Peñuelas, J., Campioli, M., 2022. Wood growth phenology and its relationship with leaf phenology in deciduous forest trees of the temperate zone of Western Europe. Agric. For. Meteorol. 327.
Fang, J., Chen, A., Peng, C., Zhao, S., Ci, L., 2001. Changes in forest biomass carbon storage in China between 1949 and 1998. Science 292 (5525), 2320–2322.
FAO, 2020. Global Forest Resources Assessment 2020. Food and Agriculture Organization of the United Nations.
Fei, S., Desprez, J.M., Potter, K.M., Jo, I., Knott, J.A., Oswalt, C.M., 2017. Divergence of species responses to climate change. Sci. Adv. 3 (5), e1603055.
Fonti, P., von Arx, G., Garcia-Gonzalez, I., Eilmann, B., Sass-Klaassen, U., Gartner, H., Eckstein, D., 2010. Studying global change through investigation of the plastic responses of xylem anatomy in tree rings. N. Phytol. 185 (1), 42–53.
Fritts, H.C., 1962. The relation of growth ring widths in American beech and white oak to variations in climate.
Gao, J., Yang, B., Peng, X., Rossi, S., 2021. Tracheid development under a drought event producing intra-annual density fluctuations in the semi-arid China. Agric. For. Meteorol. 308-309.
García-Cervigón, A.I., Camarero, J.J., Espinosa, C.I., 2017. Intra-annual stem increment patterns and climatic responses in five tree species from an Ecuadorian tropical dry forest. Trees 31 (3), 1057–1067.
García-González, I., Souto-Herrero, M., Campelo, F., 2016. Ring-porosity and earlywood vessels: a review on extracting environmental information through time. Iawa J. 37 (2), 295–314.
Gricar, J., Jevsenak, J., Hafner, P., Prislan, P., Ferlan, M., Lavric, M., Vodnik, D., Eler, K., 2022. Climatic regulation of leaf and cambial phenology in Quercus pubescens: Their interlinkage and impact on xylem and phloem conduits. Sci. Total Environ. 802, 149968.
Gričar, J., Zupančič, M., Čufar, K., Koch, G., Schmitt, U., Oven, P., 2006. Effect of local heating and cooling on cambial activity and cell differentiation in the stem of Norway spruce (Picea abies). Ann. Bot. 97 (6), 943–951.
Grotta, A., Gartner, B.L., Radosevich, S., Huso, M., 2005. Influence of red alder competition on cambial phenology and latewood formation in Douglas-fir. Iawa J. 26 (3), 309–324.
Gruber, A., Wieser, G., Oberhuber, W., 2009. Intra-annual dynamics of stem CO2 efflux in relation to cambial activity and xylem development in Pinus cembra. Tree Physiol. 29 (5), 641–649.
Hansen, A.J., Neilson, R.P., Dale, V.H., Flather, C.H., Iverson, L.R., Currie, D.J., Shafer, S., Cook, R., Bartlein, P.J., 2001. Global change in forests: responses of species, communities, and biomes: interactions between climate change and land use are projected to cause large shifts in biodiversity. BioScience 51 (9), 765–779.
Huang, J.G., Deslauriers, A., Rossi, S., 2014. Xylem formation can be modeled statistically as a function of primary growth and cambium activity. N. Phytol. 203 (3), 831–841.
Huang, J.G., Ma, Q., Rossi, S., Biondi, F., Deslauriers, A., Fonti, P., Liang, E., Makinen, H., Oberhuber, W., Rathgeber, C.B.K., Tognetti, R., Treml, V., Yang, B., Zhang, J.L., Antonucci, S., Bergeron, Y., Camarero, J.J., Campelo, F., Cufar, K., Cuny, H.E., De Luis, M., Giovannelli, A., Gricar, J., Gruber, A., Gryc, V., Guney, A., Guo, X., Huang, W., Jyske, T., Kaspar, J., King, G., Krause, C., Lemay, A., Liu, F., Lombardi, F., Martinez Del Castillo, E., Morin, H., Nabais, C., Nojd, P., Peters, R.L., Prislan, P., Saracino, A., Swidrak, I., Vavrcik, H., Vieira, J., Yu, B., Zhang, S., Zeng, Q., Zhang, Y., Ziaco, E., 2020. Photoperiod and temperature as dominant environmental drivers triggering secondary growth resumption in Northern Hemisphere conifers. PNAS 117 (34), 20645–20652.
Hunter, A.F., Lechowicz, M.J., 1992. Predicting the timing of budburst in temperate trees. J. Appl. Ecol. 597–604.
Kark, S., 2013. Ecotones and Ecological Gradients. In: Leemans, R. (Ed.), Ecological Systems: Selected Entries from the Encyclopedia of Sustainability Science and Technology. Springer New York, New York, NY, pp. 147–160.
Kitin, P., Funada, R., 2016. Earlywood vessels in ring-porous trees become functional for water transport after bud burst and before the maturation of the current-year leaves. Iawa J. 37 (2), 315–331.
Kudo, K., Utsumi, Y., Kuroda, K., Yamagishi, Y., Nabeshima, E., Nakaba, S., Yasue, K., Takata, K., Funada, R., 2018. Formation of new networks of earlywood vessels in seedlings of the deciduous ring-porous hardwood Quercus serrata in springtime. Trees 32 (3), 725–734.
Lenoir, J., Gegout, J.C., Marquet, P.A., de Ruffray, P., Brisse, H., 2008. A significant upward shift in plant species optimum elevation during the 20th century. Science 320 (5884), 1768–1771.
Li, W., Manzanedo, R.D., Jiang, Y., Ma, W., Du, E., Zhao, S., Rademacher, T., Dong, M., Xu, H., Kang, X., Wang, J., Wu, F., Cui, X., Pederson, N., 2023. Reassessment of growth-climate relations indicates the potential for decline across Eurasian boreal larch forests. Nat. Commun. 14 (1), 3358.
Linares, J.C., Camarero, J.J., Carreira, J.A., 2009. Interacting effects of changes in climate and forest cover on mortality and growth of the southernmost European fir forests. Glob. Ecol. Biogeogr. 18 (4), 485–497.
Liu, S., Li, X., Rossi, S., Wang, L., Li, W., Liang, E., Leavitt, S.W., 2018. Differences in xylogenesis between dominant and suppressed trees. Am. J. Bot. 105 (5), 950–956.

Martin-Benito, D., Pederson, N., Svenning, J.C., 2015. Convergence in drought stress, but a divergence of climatic drivers across a latitudinal gradient in a temperate broadleaf forest. J. Biogeogr. 42 (5), 925–937.
Martinez del Castillo, E., Longares, L.A., Gričar, J., Prislan, P., Gil-Pelegrín, E., Čufar, K., De Luis, M., 2016. Living on the edge: contrasted wood-formation dynamics in Fagus sylvatica and Pinus sylvestris under Mediterranean conditions. Front. Plant Sci. 7, 370.
Martinez-Sancho, E., Dorado-Linan, I., Hacke, U.G., Seidel, H., Menzel, A., 2017. Contrasting Hydraulic Architectures of Scots Pine and Sessile Oak at Their Southernmost Distribution Limits. Front Plant Sci. 8, 598.
Miller, E.W., Rademacher, T., Fonti, P., Seyednasrollah, B., Richardson, A.D., 2022. Assessing intra-annual density fluctuations across and along white pine stems. Botany 100 (7), 583–591.
Mu, W., Wu, X., Camarero, J.J., Fu, Y.H., Huang, J., Li, X., Chen, D., 2023. Photoperiod drives cessation of wood formation in northern conifers. Glob. Ecol. Biogeogr. 32 (4), 603–617.
Oribe, Y., Funada, R., Kubo, T., 2003. Relationships between cambial activity, cell differentiation and the localization of starch in storage tissues around the cambium in locally heated stems of Abies sachalinensis (Schmidt) Masters. TreesStruct. Funct. 17 (3), 185–192.
Pan, Y., Birdsey, R.A., Fang, J., Houghton, R., Kauppi, P.E., Kurz, W.A., Phillips, O.L., Shvidenko, A., Lewis, S.L., Canadell, J.G., Ciais, P., Jackson, R.B., Pacala, S.W., McGuire, A.D., Piao, S., Rautiainen, A., Sitch, S., Hayes, D., 2011. A large and persistent carbon sink in the world's forests. Science 333 (6045), 988–993.
Popkova, M.I., Vaganov, E.A., Shishov, V.V., Babushkina, E.A., Rossi, S., Fonti, M.V., Fonti, P., 2018. Modeled tracheidograms disclose drought influence on Pinus sylvestris tree-rings structure from Siberian forest-steppe. Front. Plant Sci. 9, 1144.
Pugh, T.A.M., Rademacher, T., Shafer, S.L., Steinkamp, J., Barichivich, J., Beckage, B., Haverd, V., Harper, A., Heinke, J., Nishina, K., Rammig, A., Sato, H., Arneth, A., Hantson, S., Hickler, T., Kautz, M., Quesada, B., Smith, B., Thonicke, K., 2020. Understanding the uncertainty in global forest carbon turnover. Biogeosciences 17 (15), 3961–3989.
Quinn, G.P., Keough, M.J., 2002. Experimental design and data analysis for biologists. Cambridge University Press.
Rademacher, T., Fonti, P., LeMoine, J.M., Fonti, M.V., Bowles, F., Chen, Y., Eckes-Shephard, A.H., Friend, A.D., Richardson, A.D., 2022. Insights into source/sink controls on wood formation and photosynthesis from a stem chilling experiment in mature red maple. N. Phytol. 236 (4), 1296–1309.
Rathgeber, C.B., Rossi, S., Bontemps, J.D., 2011. Cambial activity related to tree size in a mature silver-fir plantation. Ann. Bot. 108 (3), 429–438.
Ren, P., Rossi, S., Camarero, J.J., Ellison, A.M., Liang, E., Penuelas, J., 2018. Critical temperature and precipitation thresholds for the onset of xylogenesis of Juniperus przewalskii in a semi-arid area of the north-eastern Tibetan Plateau. Ann. Bot. 121 (4), 617–624.
Ren, P., Ziaco, E., Rossi, S., Biondi, F., Prislan, P., Liang, E., 2019. Growth rate rather than growing season length determines wood biomass in dry environments. Agric. For. Meteorol. 271, 46–53.
Richardson, A.D., O'Keefe, J., 2009. Phenological differences between understory and overstory: a case study using the long-term Harvard Forest records. Phenol. Ecosyst. Process. Appl. Glob. Change Res. 87–117.
Rigling, A., Waldner, P.O., Forster, T., Bräker, O.U., Pouttu, A., 2001. Ecological interpretation of tree-ring width and intraannual density fluctuations in Pinus sylvestris on dry sites in the central Alps and Siberia. Can. J. For. Res. 31 (1), 18–31.
Rollinson, C.R., Alexander, M.R., Dye, A.W., Moore, D.J.P., Pederson, N., Trouet, V., 2021. Climate sensitivity of understory trees differs from overstory trees in temperate mesic forests. Ecology 102 (3), e03264.
Rossi, S., Anfodillo, T., Menardi, R., 2006a. Trephor: A new tool for sampling microcores from tree stems. Iawa J. 27 (1), 89–97.
Rossi, S., Deslauriers, A., Anfodillo, T., Morin, H., Saracino, A., Motta, R., Borghetti, M., 2006b. Conifers in cold environments synchronize maximum growth rate of tree-ring formation with day length. N. Phytol. 170 (2), 301–310.
Rossi, S., Deslauriers, A., Anfodillo, T., Carrer, M., 2008a. Age-dependent xylogenesis in timberline conifers. N. Phytol. 177 (1), 199–208.
Rossi, S., Deslauriers, A., Griçar, J., Seo, J.-W., Rathgeber, C.B.K., Anfodillo, T., Morin, H., Levanic, T., Oven, P., Jalkanen, R., 2008b. Critical temperatures for xylogenesis in conifers of cold climates. Glob. Ecol. Biogeogr. 17 (6), 696–707.
Rossi, S., Girard, M.J., Morin, H., 2014. Lengthening of the duration of xylogenesis engenders disproportionate increases in xylem production. Glob. Change Biol. 20 (7), 2261–2271.
Rossi, S., Anfodillo, T., Čufar, K., Cuny, H.E., Deslauriers, A., Fonti, P., Frank, D., Gricar, J., Gruber, A., Huang, J.G., Jyske, T., Kaspar, J., King, G., Krause, C., Liang, E., Makinen, H., Morin, H., Nojd, P., Oberhuber, W., Prislan, P., Rathgeber, C. B., Saracino, A., Swidrak, I., Treml, V., 2016. Pattern of xylem phenology in conifers of cold ecosystems at the Northern Hemisphere. Glob. Change Biol. 22 (11), 3804–3813.
Rudolph, A.J., Snell, R.S., Delach, E., McCarthy, B.C., 2024. Interspecific, conspecific, and ontogenetic responses of tree rings to climate: A case study utilizing Carya glabra, Carya ovata, Carya tomentosa, and Quercus montana from an Oak-Hickory Forest in Southeastern Ohio. Dendrochronologia 87, 126254.
Song, H., Zhang, X., Wang, X., Wang, Y., Li, S., Xu, Y., 2023. Not the expected poleward migration: Impact of climate change scenarios on the distribution of two endemic evergreen broad-leaved Quercus species in China. Sci. Total Environ. 889, 164273.
Sperry, J.S., Nichols, K.L., Sullivan, J.E., Eastlack, S.E., 1994. Xylem embolism in ring-porous, diffuse-porous, and coniferous trees of northern Utah and interior Alaska. Ecology 75 (6), 1736–1752.
Sullivan, P.F., Brownlee, A.H., Ellison, S.B., Cahoon, S.M., 2021. Comparative drought sensitivity of co-occurring white spruce and paper birch in interior Alaska. J. Ecol. 109 (6), 2448–2460.
Tyrgotov, A., van der Maaten, E., Gradel, A., van der Maaten-Theunissen, M., 2024. Growth responses of Persian walnut (Juglans regia L.) to climate variation along its full elevational range in Kyrgyzstan. Dendrochronologia 85.
Vieira, J., Rossi, S., Campelo, F., Nabais, C., 2014. Are neighboring trees in tune? Wood formation in Pinus pinaster. Eur. J. For. Res. 133 (1), 41–50.
Wagner, R.J., Kaye, M.W., Abrams, M.D., Hanson, P.J., Martin, M., 2012. Tree-ring growth and wood chemistry response to manipulated precipitation variation for two temperate Quercus species. Tree Ring Res. 68 (1), 17–29.
Wang, W., Huang, J.G., Zhang, T., Qin, L., Jiang, S., Zhou, P., Zhang, Y., Penuelas, J., 2023. Precipitation regulates the responses of xylem phenology of two dominant tree species to temperature in arid and semi-arid forest of the southern Altai Mountains. Sci. Total Environ. 886, 163951.
Wiles, G., Wiesenberg, N., Pollock, M., Denes, C., Cooper, T., Smith, D., Wiles, M., 2025. Changing climate response of Northeast Ohio white oaks, USA: Is it tree age or site age? Dendrochronologia 91.
Zhang, J., Gou, X., Zhao, Z., Liu, W., Zhang, F., Cao, Z., Zhou, F., 2013. Improved method of obtaining micro-core paraffin sections in Dendroecological research. Chin. J. Plant Ecol. 37 (10), 972–978.
Zhang, J., Gou, X., Manzanedo, R.D., Zhang, F., Pederson, N., 2018a. Cambial phenology and xylogenesis of Juniperus przewalskii over a climatic gradient is influenced by both temperature and drought. Agric. For. Meteorol. 260-261, 165–175.
Zhang, J., Gou, X., Pederson, N., Zhang, F., Niu, H., Zhao, S., Wang, F., 2018b. Cambial phenology in Juniperus przewalskii along different altitudinal gradients in a cold and arid region. Tree Physiol. 38 (6), 840–852.
Zhang, J., Alexander, M.R., Gou, X., Deslauriers, A., Fonti, P., Zhang, F., Pederson, N., 2020. Extended xylogenesis and stem biomass production in Juniperus przewalskii Kom. during extreme late-season climatic events. Ann. For. Sci. 77 (4), 99.
Zhang, J., Gou, X., Alexander, M.R., Xia, J., Wang, F., Zhang, F., Man, Z., Pederson, N., 2021. Drought limits wood production of Juniperus przewalskii even as growing seasons lengthens in a cold and arid environment. Catena 196, 104936.
Zhang, J., Gou, X., Rademacher, T., Wang, L., Li, Y., Sun, Q., Wang, F., Cao, Z., 2023. Interaction of age and elevation on xylogenesis in Juniperus przewalskii in a cold and arid region. Agric. For. Meteorol. 337, 109480.
Ziaco, E., Truettner, C., Biondi, F., Bullock, S., 2018. Moisture-driven xylogenesis in Pinus ponderosa from a Mojave Desert mountain reveals high phenological plasticity. Plant Cell Environ. 41 (4), 823–836.